

**GALLIUM NITRIDE (GaN) BASED GAS SENSOR  
USING CATALYTIC METAL**

**by**

**ABDO YAHYA OMER HUDEISH**

**Thesis submitted in fulfillment of the requirements  
for the degree of  
Doctor of Philosophy**

**December 2005**

## ACKNOWLEDGMENTS

Firstly and out most I am thankful to **Allah** Sobhanahu wataala. Also I would like also to express my deep gratitude to my supervisor, Dr. Azlan Abdul Aziz, for giving me the opportunity to perform this work, for his helpful assistance, priceless discussions, teaching and his righteous behavior. I also would like to sincerely thank Dr. Zainuriah Hassan, for additional advice and help. Without her patience, guidance and constant supports, this work would not have been possible.

I would like to acknowledge my family for their tireless love and support over the years. A special word of thanks goes to my brothers Ali, Omer and Adel, having made it through their words of encouragement. I would like to thank my parents and the dearest Haji Abd Arrahman Khorgeen for working hard to provide me with the best educational opportunities, for supporting all of my decisions, and for serving as the shining examples of how to live a rewarding and meaningful life. I would like thank Haji. Abd Al-Jaleel Abdo Thabet, also my thanks for all of People's General Congress (PGC) Hodeidah University and Yemen government.

Thanks also go to the offices of Universiti Sains Malaysia for example IPS, School of Physics, Dean, both deputy Deans and all the staff in the main office. Special thanks to Prof. Dr. Haji. Kamarulazizi Ibrahim for his and his friendly behavior in helping me throughout my work and to NOR laboratory assistants, Silicon laboratory assistants, all staff and all MSc and Ph.D students here. I would also like to acknowledge my friends Dr. Ibrahim Hamamu from Libya and Dr. Nihad Khalaf Ali from Iraq.

*Abdo Yahya Omer Hudeish*  
*December 2005*

# TABLE OF CONTENTS

	page
ACKNOWLEDGMENT	II
TABLE OF CONTENTS	III
TABLES CAPTIONS	VI
FIGURES CAPTIONS	VII
LIST OF SYMBOLS	XII
ABSTRAK	XV
ABSTRACT	XVII
1.0 CHAPTER [1] INTRODUCTION	1
1.1 Scope	1
1.2 General Approach to Semiconductor Gas Sensors Detection	2
1.2.1 Sensitivity	7
1.2.2 Selectivity	7
1.2.3 Stability	8
1.2.4 Smart power consumption	9
1.3 Mechanisms of gas sensing	10
1.4 Objective	11
1.5 Outline of the thesis	12
2.0 CHAPTER [2] CHEMICAL SENSORS	13
2.1 What is a sensor?	13
2.2 Liquid Sensors	14
2.3 GaN Gas Sensor	17
2.3.1 GaN Gas Sensor Science and Technology	17
2.4 GaN Gas Sensing Mechanism	18
2.4.1 Gas Mechanisms	18
2.4.2 Microstructures	21
2.4.3 Hydrogen Sensing and Transduction	23
2.4.4 Current/Voltage (I-V) Characteristics	24
2.4.5 Influence Of Different Hydrogen Concentration and its Operating Temperatures	26
2.4.6 Adsorption of Nitrogen	27
2.4.7 Detection of Methane	28
3.0 CHAPTER [3] GALLIUM NITRIDE MATERIALS TECHNOLOGY	30
3.1 Introduction	30
3.2 Materials Technology For GaN Substrates	32
3.3 Materials Growth	34
3.3.1 Metalorganic Chemical Vapor Deposition (MOCVD)	34
3.3.2 MOCVD Reaction Chemistry	34
3.3.3 MOCVD System and Reactor Design Issues	36
3.3.4 Molecular Beam Epitaxy (MBE)	37
3.3.5 GaN p-type and n-type Doping	39
3.3.6 Lateral Epitaxial Overgrowth	40
3.4 GaN High Temperature Electronics Background	41
3.5 Low Resistance Contacts to the Source and Drain	42

4.0	CHAPTER [4] CHARACTERIZATION TECHNIQUES	44
4.1	Introduction	44
4.2	General Characterization Techniques	44
4.2.1	X-Ray Diffraction	44
4.2.2	Scanning Electron Microscopy	46
4.2.3	Electron Dispersive X-ray Spectroscopy	49
4.2.4	Atomic Force Microscopy	50
4.3	Experimental Techniques	51
4.4	Sensor Electronics	53
4.5	Design and Construction of Sensor Testing Chamber	54
4.5.1	Test System	54
4.5.2	Gas Flow in the Testing Chamber	56
4.6	Controlling the Surface Temperature	57
4.7	Electrical Measurements	58
4.8	Data Acquisition System	60
4.9	Studying Sensor Performance	60
4.9.1	Resistance Response Ratio	60
4.9.2	Response and Recovery Times	62
5.0	CHAPTER [5] PERFORMANCE PROPERTIES OF GaN FOR GAS SENSORS	63
5.1	Introduction	63
5.2	Experimental Procedure	63
5.3	Electrical Characterization	64
5.3.1	Gas Sensor Based On Pt/n-GaN	64
5.3.1.1	Nitrogen Detection	64
5.3.1.2	Hydrogen Detection	66
5.3.1.3	Methane Detection	69
5.3.1.4	Conclusions	71
5.3.2	Gas Sensor Based On Pd/n-GaN	71
5.3.2.1	Nitrogen Detection	71
5.3.2.2	Hydrogen Detection	73
5.3.2.3	Methane Detection	76
5.3.2.4	Conclusions	77
5.3.3	Gas Sensor Based On Ag/n-GaN	78
5.3.3.1	Nitrogen Detection	78
5.3.3.2	Hydrogen Detection	80
5.3.3.3	Methane Detection	82
5.3.3.4	Conclusions	84
5.3.4	Gas Sensor Based On Ni/n-GaN	84
5.3.4.1	Nitrogen Detection	84
5.3.4.2	Hydrogen Detection	87
5.3.4.3	Methane Detection	89
5.3.4.4	Conclusions	91
5.4	Gas Sensor Based On p-GaN and n-AlGa <sub>N</sub>	91
5.4.1	Gas Sensor Based On p-GaN	91
5.4.2	Gas Sensor Based On n-AlGa <sub>N</sub> .	94
5.5	Current-Voltage (I-V) Characterization and Schottky barrier heights SBH	96
5.6	Discussion and Conclusions	112

5.6.1	Sensor Resistance in Air	112
5.6.2	Sensor Response Gases Exposure	113
5.6.2.1	Nitrogen Sensor Response	113
5.6.2.2	Hydrogen Sensor Response	115
5.6.2.3	Methane Sensor Response	119
5.6.2.4	I-V Characteristics and Barrier Height	122
5.7	Conclusion	123
6.0	CHAPTER [6] SURFACE MORPHOLOGY OF GaN BASED GAS SENSOR	124
6.1	Introduction	124
6.2	Structural Evolution of GaN Based Gas Sensor	124
6.2.1	Influence of Grain Size	125
6.2.2	Surface Morphology and Interfacial Reaction	128
6.2.2.1	Energy-Dispersive Spectroscopy (EDS) Results	128
6.2.2.2	Scanning Electron Microscopy (SEM) Results	131
6.2.2.3	Atomic Force Microscopy (AFM) Results.	135
6.2.3	Microstructural Analysis Based on X-ray Diffraction (XRD) Results.	138
6.3	Discussion	142
6.3.1	Interfacial Reactions and Microstructure	142
6.3.2	Correlation Between Electrical Properties of Contacts and Microstructures	143
6.4	Conclusions	144
7.0	CHAPTER [7] CONCLUSIONS AND OUTLOOK	146
7.1	Conclusions	146
7.2	Overview Of Future Work	152
	REFERENCES	153
	PAPERS PUBLISHED AND CONFERENCES	167

## TABLES CAPTIONS

	Page
Table 2.1 Properties of semiconductors (Pearson et al., 2002).	18
Table 4.1 Samples with different parameters of (annealing temperature, metal thickness and gases exposure.)	52
Table 5.1 The absolute of Barrier height ( $\phi_B$ ) for Pt/n-GaN upon exposure of air, N <sub>2</sub> , 10% H <sub>2</sub> in N <sub>2</sub> and CH <sub>4</sub> ambient as a function of measurement temperature.	107
Table 5.2 The absolute of Barrier height ( $\phi_B$ ) for Pt/p-GaN upon exposure of air, N <sub>2</sub> , 5% H <sub>2</sub> in N <sub>2</sub> and CH <sub>4</sub> ambient as a function of measurement temperature.	107
Table 5.3 The absolute of Barrier height ( $\phi_B$ ) for Pt/AlGaIn upon exposure of air, N <sub>2</sub> , 2% H <sub>2</sub> in N <sub>2</sub> and CH <sub>4</sub> ambient as a function of measurement temperature.	107
Table 5.4 Selected characteristics of gas sensors based on Pt/ n-GaN, Pd/ n-GaN, Ag/ n-GaN and Ni/ n-GaN with N <sub>2</sub> exposure.	114
Table 5.5 Selected characteristics of gas sensors based on Pt/ n-GaN, Pd/ n-GaN, Ag/ n-GaN, Ni/ n-GaN, Pt/p-GaN, Pt/p-GaN Pt/AlGaIn and Pt/AlGaIn with H <sub>2</sub> exposure.	118
Table 5.6 Selected characteristics of gas sensors based on Pt/ n-GaN, Pd/ n-GaN, Ag/ n-GaN and Ni/ n-GaN with CH <sub>4</sub> exposure.	121
Table 6.1 XRD pictograph of n-GaN based sensor grain size for samples as deposited and after annealed at 600°C upon hydrogen exposure.	142
Table 7.1 Selected characteristics of gas sensors based on Pt/ n-GaN, Pd/ n-GaN, Ag/ n-GaN and Ni/ n-GaN with N <sub>2</sub> , H <sub>2</sub> and CH <sub>4</sub> exposure.	146

## FIGURES CAPTIONS

		page
Fig. 1.1	Simple scheme of SGS with Si substrate, electrodes and heater resistance (Cirera, 2000).	6
Fig. 1.2	Gas sensor system that includes electronics for signal processing [Figaro, 2000].	6
Fig. 2.1	This bottle contains both liquid bromine [ $\text{Br}_2(\text{l})$ , the darker phase at the bottom of the bottle] and gaseous bromine [ $\text{Br}_2(\text{g})$ , the lighter phase above the liquid]. The circles show microscopic views of both liquid bromine and gaseous bromine.	15
Fig. 2.2	Energy band gap for semiconductors (Pearson et al., 2002).	18
Fig. 2.3	Fig. 2.4: Proposed gas sensing mechanisms underlying the function of catalytic metal gas sensor devices ( $\text{H}_{\text{ads}}$ , $\text{H}_i$ : adsorbed and interfacial hydrogen; $\text{X}_{\text{ads}}$ , $\text{X}_i$ : adsorbed and interfacial molecules).	21
Fig. 2.4	Schematic representation of (a) porous and (b) compact sensing layer with geometry and energy band. $x_g$ grain size, $L_D$ Debye length, $eV_s$ band bending, $z_0$ thickness of the depleted surface layer and $z_g$ layer thickness (Simon et al., 2001).	22
Fig. 2.5	Schematic representation of a porous sensing layer with geometry and energy band. $\lambda_D$ is the Debye length, $x_g$ is the grain size and $x_0$ is the depth of the depletion layer (Barsan & Weimar, 2003; 2001).	24
Fig. 3.1	Bandgap and Wavelength of III-V Nitrides versus Lattice Constant (Weeks et al. 1995).	33
Fig. 3.2	Typical arrangement for metal-organic chemical vapor deposition (MOCVD) machine (Miller, 2000).	37
Fig. 3.3	Schematic diagram of molecular beam epitaxy (MBE) system (Miller, 2000).	38
Fig. 4.1	Bragg law (Cullity, 1989).	45
Fig. 4.2	Block diagram of a typical SEM ( <a href="http://www.forensicevidence.net">http://www.forensicevidence.net</a> )	47
Fig. 4.3	An illustration of the classical models showing the production of Bremsstrahlung, characteristic X-rays, and Auger electrons.	48
Fig. 4.4	EDS spectrum of a specimen containing Ga, Pt and $\text{O}_2$ . ( <a href="http://www.thebritishmuseum.ac.uk">http://www.thebritishmuseum.ac.uk</a> ).	50

Fig. 4.5	Contact electrode of GaN gas sensor.	52
Fig. 4.6	Block diagram of the constant current, constant voltage sensor drive circuit.	53
Fig. 4.7	Home made sensor chamber connected at computerized I-V and gas exposure.	55
Fig. 4.8	Schematic diagram for GaN gas sensors measurement. $V_C$ : circuit voltage; $V_H$ : heater voltage; $R_L$ : load resistance; $V_{RL}$ : output voltage; $R_S$ : GaN resistance (Dae-Sik <i>et al.</i> , 2003).	55
Fig. 4.9	Experimental setup of the system used to test gas sensitivity.	56
Fig. 4.10	Diagram of the setup used to measure the resistance and heat the samples.	57
Fig. 4.11	Schematic diagram of the testing chamber used for sensor characteristics measurement.	59
Fig. 5.1	Sensor response of 600 and 900°C annealed Pt/ n-GaN to $N_2$ at different operating temperatures.	65
Fig. 5.2	Variation of 600°C-annealed Pt/ n-GaN sensor resistance to a pulse of nitrogen for different operating temperatures.	65
Fig. 5.3	Variation of 900°C-annealed Pt/ n-GaN sensor resistance to a pulse of nitrogen for different operating temperatures.	66
Fig. 5.4	Sensor response of 600 and 900°C annealed Pt/ n-GaN to 2% $H_2$ in $N_2$ in at different operating temperatures.	67
Fig. 5.5	Variation of the 600°C and 900°C annealed Pt/ n-GaN - based sensor resistance under a pulse of 2% $H_2$ in $N_2$ .	67
Fig. 5.6	Sensor response of 600°C and 900°C annealed Pt/ n-GaN to different concentrations of $H_2$ at 250°C.	68
Fig. 5.7	Sensor response of 600°C and 900°C annealed Pt/ n-GaN to different concentrations of $H_2$ in $N_2$ .	68
Fig. 5.8	Sensor response of 600°C and 900°C annealed Pt/ n-GaN to $CH_4$ at different operating temperatures.	70
Fig. 5.9	Variation of the 600°C and 900°C annealed Pt/ n-GaN - based sensor resistance under a pulse of different concentration of $CH_4$ at 250°C.	70
Fig. 5.10	Sensor response of 600°C and 900°C annealed Pd/ n-GaN to $N_2$ at different operating temperatures.	72
Fig. 5.11	Variation of 600°C and 900°C annealed Pd/ n-GaN sensor resistance to a pulse of nitrogen at 300°C.	72

Fig. 5.12	Sensor response of 600°C and 900°C annealed Pd/ n-GaN to 2% H <sub>2</sub> in N <sub>2</sub> at different operating temperatures.	74
Fig. 5.13	Sensor response of 600°C and 900°C annealed Pd/ n-GaN to different concentrations of H <sub>2</sub> at 250°C.	74
Fig. 5.14	Sensor response of 600°C and 900°C annealed Pd/ n-GaN to different concentrations of H <sub>2</sub> in N <sub>2</sub> .	75
Fig. 5.15	Sensor response of Pd/ n-GaN to CH <sub>4</sub> at different operating temperatures.	76
Fig. 5.16	Dynamic sensor response of 600°C and 900°C annealed Pd/ n-GaN sensor resistance to a pulse of methane at 300°C.	77
Fig. 5.17	Sensor response of 600°C and 900°C annealed Ag/ n-GaN to N <sub>2</sub> at different operating temperatures.	79
Fig. 5.18	Sensor response of 600°C and 900°C annealed Ag/ n-GaN to different thickness of Ag to N <sub>2</sub> at different operating temperatures.	79
Fig. 5.19	Sensor response of 600°C and 900°C annealed Ag/ n-GaN between air and N <sub>2</sub> at 200°C.	80
Fig. 5.20	Sensor response of 600°C and 900°C annealed Ag/ n-GaN to different concentration of H <sub>2</sub> in nitrogen at different operating temperatures.	81
Fig. 5.21	Sensor response of 600°C and 900°C annealed Ag/ n-GaN to 10% of H <sub>2</sub> in N <sub>2</sub> at different operating temperatures.	82
Fig. 5.22	Sensor response of 600°C and 900°C annealed Ag/ n-GaN to CH <sub>4</sub> at different operating temperatures.	83
Fig. 5.23	Sensor response of 600°C annealed Ag/ n-GaN to different concentration of CH <sub>4</sub> at different operating temperatures.	83
Fig. 5.24	Sensor response of 600°C and 900°C annealed Ni/ n-GaN to N <sub>2</sub> at different operating temperatures.	86
Fig. 5.25	Variation of 900°C annealed Ni/ n-GaN sensor resistance to a pulse of nitrogen for different operating temperatures.	86
Fig. 5.26	Dynamic sensor response of 900°C annealed Ni/ n-GaN to air and nitrogen at 300°C.	87
Fig. 5.27	Sensor response of 600°C and 900°C annealed Ni/ n-GaN 100 and 200 nm to 2% H <sub>2</sub> in N <sub>2</sub> at different operating temperatures.	88
Fig. 5.28	Sensor resistance of 100nm thickness of Ni/ n-GaN annealed at 600°C and 900°C for different concentrations of H <sub>2</sub> in N <sub>2</sub> at 200°C operating temperature.	89

Fig. 5.29	Sensor response of 600°C-annealed Ni/ n-GaN (100 and 200 nm) to different concentration of CH <sub>4</sub> at different operating temperatures.	90
Fig. 5.30	Dynamic sensor response of 600°C and 900°C annealed Ni/ n-GaN to CH <sub>4</sub> at operating temperature of 300°C.	90
Fig. 5.31	Sensor response of 600°C and 900°C annealed Pt/p-GaN and Ni/p-GaN to 2%H <sub>2</sub> in N <sub>2</sub> at different operating temperatures.	93
Fig. 5.32	Sensor response of 600°C and 900°C annealed Pt/p-GaN upon pure N <sub>2</sub> and to different concentrations of H <sub>2</sub> in N <sub>2</sub> exposure.	93
Fig. 5.33	Sensor response of 600°C and 900°C annealed Pt/AlGaIn and Ni/AlGaIn to 2%H <sub>2</sub> in N <sub>2</sub> at different operating temperatures.	95
Fig. 5.34	Sensor response of 600°C and 900°C annealed Pt/p-GaN upon pure N <sub>2</sub> and to different concentrations of H <sub>2</sub> in N <sub>2</sub> exposure.	95
Fig. 5.35	Typical Curve of ln I versus V (Dieter and Schroder, 1990).	97
Fig. 5.36	Low forward bias <i>I-V</i> characteristics from Pt/n-GaN sensor in pure N <sub>2</sub> , 10% H <sub>2</sub> in N <sub>2</sub> or CH <sub>4</sub> at 200°C.	99
Fig. 5.37	Low forward bias <i>I-V</i> characteristics from Pt/n-GaN, Pt/p-GaN and Pt/n-AlGaIn sensors in 10 %H <sub>2</sub> in N <sub>2</sub> at 200°C.	100
Fig. 5.38	Forward-bias <i>I-V</i> characteristics of Ni/p-GaN and Ni/AlGaIn upon CH <sub>4</sub> at 25°C and 100°C	100
Fig. 5.39	Forward-bias <i>I-V</i> characteristics of Ni/AlGaIn at 100°C in air, pure N <sub>2</sub> , and in N <sub>2</sub> containing hydrogen between 2% to 10%.	101
Fig. 5.40	Forward <i>I-V</i> characteristics from Pd/n-GaN diodes measured at 50°C or 350°C in N <sub>2</sub> or 10% H <sub>2</sub> in N <sub>2</sub> ambients.	102
Fig. 5.41	Forward <i>I-V</i> characteristics from Pt/n-GaN, Pd/n-GaN Ni/n GaN and Ag/n- GaN sensors measured at 25°C N <sub>2</sub> or 2% H <sub>2</sub> in N <sub>2</sub> ambients.	103
Fig. 5.42	<i>I-V</i> Characteristic of Ni/n-GaN at operating temperature 200 °C.	103
Fig. 5.43(a)	Plot of ln I versus V of Ni/n-GaN at operating temperature 200 °C.	104
Fig. 5.43(b)	Plot of ln I versus V of Ni/n-GaN at operating temperature 200 °C.	104

Fig. 5.44	Plot of experimental of change in barrier height ( $\Phi_B$ ) vs. temperature of Ni/AlGaN Schottky barrier with gases exposure.	110
Fig. 5.45	Plot of experimental of change in barrier height ( $\Phi_B$ ) vs. temperature of Pt/p-GaN Schottky barrier with gases exposure.	110
Fig. 5.46	Plot of experimental of change in barrier height ( $\Phi_B$ ) vs. temperature of Pt/AlGaN, Pt/p-GaN, Pt/n-GaN Schottky barrier with gases exposure.	111
Fig. 5.47	Variation of sensor resistance in air as a function of operating temperature for Pt/n-GaN, Pd/n-GaN, Ag/n-GaN and Ni/n-GaN based sensors.	112
Fig. 6.1	Scanning electron microscope images of the samples a) Pt/ n-GaN and b) Ag/ n-GaN.	126
Fig. 6.2	AFM surface plots of samples a) Pt/ n-GaN and b) Ag/ n-GaN.	127
Fig. 6.3 (a)	SEM images of surface morphology observation of sample surface for as deposited and 600°C annealed samples for Pt and Pd with hydrogen exposure.	129
Fig. 6.3 (b)	EDS line scans taken across the contact/ n-GaN interface for Ag and Ni contacts annealed at 600°C.	130
Fig. 6.4 (a)	SEM images of surface morphology observation of sample surface contact/ n-GaN interface for as deposited Pt and Pd at 600°C annealed samples with hydrogen exposure.	133
Fig. 6.4 (b)	SEM images of surface morphology observation of sample surface for as deposited and 600°C annealed samples for Ag and Ni with hydrogen exposure.	134
Fig. 6.5	AFM morphology in 2D of Pt/ n-GaN annealed samples with nitrogen, hydrogen and methane exposure at 600°C and operating temperature of 250°C.	137
Fig. 6.6	AFM morphology in 3D of contact/ n-GaN observation of sample surface as deposited and 600°C annealed samples for Pt, Pd, Ag and Ni with hydrogen exposure.	138
Fig. 6.7	Roughness variation of sensor samples as deposited and 600°C annealed with H <sub>2</sub> exposure as found using AFM technique.	139
Fig. 6.8 (a)	XRD spectra of Pt/ n-GaN and Pd/ n-GaN samples annealed at 600°C with hydrogen exposure.	142
Fig. 6.8 (b)	XRD spectra of Ag/ n-GaN and Ni/ n-GaN samples annealed at 600°C with hydrogen exposure.	143

## LIST OF SYMBOLS

### *Abbreviations*

AFM	Atomic Force Microscopy.
Ag	Silver
CH <sub>4</sub>	Methane
CVD	Chemical Vapour Deposition.
Ct	coefficient of temperature resistance.
DC	Direct Current.
ECR	electron cyclotron resonance
EDS	Energy Dispersive Spectroscopy.
EDX	Energy Dispersive X-ray analysis.
FET	Field Effect Transistor.
FWHM	Full Width at Half Maximum.
GaN	Gallium Nitride
GaNGS	Gallium Nitride Gas Sensor
H <sub>2</sub>	Hydrogen
HPRC	high pressure research center
LED	Light Emitting Diode.
LEEBI	low electron beam irradiation
LEO	lateral epitaxial overgrowth
LNG	liquefied natural gas
MBE	Molecular Beam Epitaxy.
MCA	multi-channel analyser
MESFET	metal semiconductor field effect transistor
MIS	metal-insulator-semiconductor
MOCVD	Metalorganic Chemical Vapour Deposition.
MOS	Metal-Oxide-Semiconductor
MOSFETs	metal-oxide-semiconductor field effect transistors
MODFET	modulation doped field effect transistor
MRLS	multiple rocket launch system
MS	metal semiconductor
μ-TAS	Micro-Total Analytical Systems
N <sub>2</sub>	Nitrogen
Ni	Nickel
Pd	Palladium
Pt	Platinum
PVD	Physical Vapour Deposition.
RIE	reactive ion etching
RTA	rapid thermal annealing
SAW	Surface Acoustic Wave.
SB	Schottky Barrier
SBH	Schottky Barrier Height
SEM	Scanning Electron Microscopy.
SGS	semiconductor gas sensor
SQW	single quantum well
TD	threading dislocation
UHV	Ultra High Vacuum.
USM	Universiti Sains Malaysia
WBG	Wide bandgap
WDX	Wavelength Dispersive X-ray analysis.
XRD	X-Ray Diffraction.

### *Roman Symbols:*

A Contact aria

$A^*$	Effective Richardson coefficient
$C_g$	gas concentration.
$C_q$	flow coefficient of a valve.
$C_{(ads)}$	Carbon adsorption
$CO_{(ads)}$	Monoxide carbide adsorption
$CO_{(gas)}$	Monoxide carbide gas
$CH_{3(ads)}$	Ammonia adsorption
$CH_{4(phys)}$	Methane physisorption
$CH_{4(gas)}$	Methane gas
$CO_{2(gas)}$	Carbon dioxide gas
$d$	film thickness.
$D$	grain size
$D_{gr}$	average crystallite diameter
$G_0$	film conductance in air.
$G_S[C_g]$	conductance under a $C_g$ concentration of the gas.
$H$	Plank's constant
$H_{(ads)}$	Hydrogen adsorption
$H_i$	Hydrogen interfacial
$I$	electric current.
$I_{sat}$	Current saturation
$J_{sat}$	Current density saturation
$k$	Boltzmann constant.
$K_j$	sensitivity coefficient of reducing gas j.
$N$	number of particles.
$N_C$	Density of states in conduction band
$N_S$	amount of surface atoms
$N_V$	over bulk atoms
$O_{(ads)}$	Oxygen adsorption
$O_{(Latt)}$	Oxygen lattice
$O_0$	Oxygen site
$P$	pressure.
$q$	Electron charge
$r$	depth of external shell of atoms
$R_0$	resistance in clean air.
$R_i$	multimeter internal resistance.
$R_L$	Load resistance
$R_R$	reference resistance.
$R_S$	sample resistance.
$R_S[C_g]$	resistance under a $C_g$ concentration of the gas.
$R_{air}$	resistance of air
$R_{H_2}$	resistance of hydrogen
$R_{N_2}$	resistance of nitrogen
$R_{CH_4}$	resistance of methane
$T$	Absolute temperature
$T_a$	high-temperature post-implantation annealing steps
$T_i$	high-temperature implantation
$V$	volume
$V$	Voltage
$V_{bi}$	Built-in potential
$V_C$	Circuit voltage
$V_H$	Heater voltage
$V_{RL}$	Output voltage
$X_a$	adsorbed molecules
$X_i$	interfacial molecules

*Greek Symbols:*

$\beta$

$\lambda$

$\rho_x$

$\theta$

$\theta_B$

$\phi_B$

$\Phi_m$

$\chi_s$

$\eta$

Full Width at Half Maximum FWHM

Wavelength.

X-ray density.

angle between the radiation and the surfaces

Bragg diffraction angle.

Barrier height

Work function

Electron affinity

Ideality factor

# PENGESAN GAS BERASASKAN GALIUM NITRIDA (GaN) MENGUNAKAN LOGAM MANGKINAN

## ABSTRAK

Dalam kajian ini, Pt, Pd, Ag dan Ni dimendapkan ke atas GaN dan AlGaN jenis p dan jenis n sebagai sentuhan logam mangkinan dengan menggunakan sistem percikan menerusi topeng logam bagi mengesan gas  $N_2$ ,  $H_2$  dan  $CH_4$  dengan kepekatan dan ketebalan logam yang berbeza dalam julat dari 50 hingga 300nm. Kemudian, sampel diberi terma yang berbeza dari 500-1000°C selama 5 minit dalam gas argon bagi ciri pengesanan. Kebolehan pengesanan pengesan gas diuji dalam kebuk yang telah direka dan dibina khas. Kesemua sampel diuji dari sudut pencirian keelektrikannya dengan menggunakan kaedah arus-voltan (I-V) pada julat suhu antara 25 °C hingga 500°C. Kesemua sampel didapati mampu mengesan gas pada julat suhu yang besar di antara 25 °C hingga 500°C. Didapati bahawa pengesanan ini berupaya untuk berfungsi dalam lingkungan suhu yang luas iaitu dari 25 °C hingga 500°C.. Rintangan sampel diukur dengan parameter yang berbeza, seperti ketebalan, rawatan haba, jenis gas dan kepekatan serta such operasi. Semua rintangan sampel, masa tindak balas dan masa pulih diukur pada julat suhu yang berbeza (25 °C -500°C). Suhu rawatan haba mamainkan peranan penting dalam perbuahaan kepekaan yang mara berkaitan dengan perubahan parameter seperti logam esrta formasi dwikutub. Perubahan pada arus meningkat dengan pengukuran suhu dan bermula sejurus selepas hidrogen dibekakan. Pt/AlGaN jenis n menunjukkan peranti yang mempunyai pemilihan yang bagus kesensitifan yang tinggi apabila pengesan gas hidrogen dibandingkan dengan Pt/GaN jenis n setiap satu. Struktur logam/GaN dan lapisan filemzarah nano yang sensitif dikenalpasti menggunakan pembelaun sinar-X (XRD), mikroskopi pengimbas electron (SEM) dan mikraskopi daya atomik (AFM). Semua teknik pencirian memberikan perhubungan yang baik antara kekasaran permukaan, struktur saiz

butiran dan serapan keluar atau masuk pada prestasi pengesanan oleh pengesan logam. Data mikrostruktur dari XRD menunjukkan platinum yang nipis mempunyai ketumpatan sempadan butiran yang tinggi. Peningkatan dalam kepekaan dengan suhu operasi dan peratusan gas akan meningkatkan pemisahan molekul-molekul hidrogen pada permukaan, serapan atom hidrogen sepanjang sempadan permukaan butiran dan serapan hidrogen pada permukaan logam/GaN jenis n sebagai mekanisme yang mungkin untuk mengesan hidrogen oleh jurang Schottky. Ciri pengesan dikaji menggunakan pengukuran rintangan terhadap pendedakan gas. Filem dari platinum menunjukkan kepekaan yang tinggi terhadap gas hidrogen, pemilikan yang baik terhadap kepekatan hidrogen yang berbeza, masa tindak balas yang singkat dan masa pulih yang sesuai. Filem Pt juga menunjukkan kebolehan untuk mengesan nitrogen dan metana. Peranti ini menunjukkan kemampuan untuk aplikasi yang memerlukan kepekaan pengesanan secara jangka masa panjang yang stabil terhadap gas mudah terbakar.

# GALLIUM NITRIDE (GaN) BASED GAS SENSOR USING CATALYTIC METAL

## ABSTRACT

In this work, Pt, Pd, Ag and Ni were deposited on p type and n type of GaN and AlGaN as catalytic metals contact using sputtering system through metal mask to detect N<sub>2</sub>, H<sub>2</sub> and CH<sub>4</sub> gases with different concentrations and different metal thicknesses with a range of 50-300nm. Samples were annealed at various temperatures from 500°C up to 1000°C for 5 min in argon prior to sensing characterization. Special chamber was designed and built to test the sensor capability. All samples were examined by electrical characterization, using current-voltage (I-V) with temperature range from 25°C to 500°C. All samples were found capable of detecting gas at a broad temperature range from 25°C to 500°C. The resistance of samples was measured with different parameters such as thickness, annealing temperatures, gases, and concentration of gases and operated temperatures. All resistance of the samples, time response and recovery time were measured at different temperature range (25°C-500°C). The annealing temperature plays an important role in the changes of sensitivity due to changes of parameter such as distance between grains, outdiffusion or indiffusion of metals, and formation of dipoles. The change in current increases with measurement temperature and begins immediately upon introduction of the hydrogen. Pt/n-AlGaN showed a good device selectivity and high sensitivity as hydrogen gas sensor compared to Pt/p-GaN and Pt/n-GaN respectively. The structure of the metal/GaN and sensitive layer of the nanoparticle films was determined using X-ray diffraction (XRD), scanning electron microscopy (SEM), energy dispersive spectroscopy (EDS) and atomic force microscopy (AFM). All characterization techniques provide good correlation between surface roughness, grains size structure,

and outdiffusion or indiffusion of metal sensor sensing performance. Data from XRD of the microstructure showed that the thinner Platinum had a higher grain boundary density. The increase in sensitivity with operating temperatures and percentage of gas increases the dissociation of molecular hydrogen on the surface, the diffusion of atomic hydrogen along the surface grain boundaries and the adsorption of hydrogen at the metals/n-GaN surface as a possible mechanism of sensing hydrogen by Schottky barriers. Sensor properties were investigated using resistance measurements upon gas exposures. The films of platinum showed high sensitivity to hydrogen gas, excellent selectivity to different concentration of hydrogen, short time response and suitable recovery time. Also Pt films showed capable to detect the nitrogen and methane. These devices look promising for applications requiring sensitive, long-term stable detection of combustion gases.

# CHAPTER [1] INTRODUCTION

## 1.1 Scope

Gases are materials constituted by atoms or molecules in continuous motion with random orientation. The average distance between particles in gas phase is much wider than the typical interatomic distances inside a molecule, so that the interactions with each other are much reduced. In an ideal gas, these interactions are perfectly elastic collisions. The pressure,  $P$ , the number of particles,  $N$ , the temperature,  $T$ , and the volume,  $V$ , of an ideal gas are related by a simple formula, the ideal gas equation:  $PV = NkT$ , where  $k$  is the Boltzmann constant. In nature, however, a perfect or ideal gas can hardly be found. Real gases show deviations from this law, due mainly to the non-elastic character of the interactions.

Air, for instance, is a mixture of several gases whose main components are nitrogen and oxygen. Other components of air usually showing small concentrations are argon, other inert gases, carbon dioxide and hydrogen. The composition of air is constantly varying due to the interchange of atoms and molecules between air and the surrounding bodies and also, because of the diffusion and interaction of the particles in the gas phase. This makes the atmosphere a fully open system, spatially inhomogeneous and with rich internal dynamics. One of the compounds whose concentration shows a higher variation in air is water vapour. Other substances usually detected in varying concentrations are ozone, carbon monoxide, sulphur or nitrogen oxides and several organic volatile compounds. Also important to note is that very small solid (smoke, dust) or liquid particles (the clouds, the fog) can be carried in suspension by air.

Since air acts as a source of substances for biological processes, the absence of some of its components or the presence of unusual compounds can severely disturb the processes that depend upon it. That is the case when concentration of oxygen has been highly reduced locally in a combustion process or when a toxic compound is carried in air. Since oxygen is odourless, its shortage in atmosphere can only be perceived by the side effects on the respiratory processes. Other gaseous compounds can sometimes be perceived by smell, but in many cases they are also odourless

Natural odours are usually composed by complex mixtures of small organic molecules with relative molecular masses (Dodd *et al.*, 1992) that are carried by air along with many other chemical compounds. The odour properties, including perceived intensity, of a molecule depend on the shape, the size and the characteristics of the polar group, so that a low volatility species can be sensed intensely, while another present in high concentration can have only a low intensity smell. Olfaction may recognize a harmful substance, but more frequently it will be sensitive to natural and harmless compounds resulted from biological processes.

Gas chemical sensors respond to the presence of gases. Ideally, one would prefer to use selective sensors, with each sensor responding to the presence of a unique gas. In reality, gas chemical sensors respond to a multiple of gases. For example, the resistance of metal oxide sensors can be altered due to changes in the concentrations of O<sub>2</sub>, CO, CO<sub>2</sub>, H<sub>2</sub>, CH<sub>4</sub>, and other hydrocarbons.

## **1.2 General Approach to Semiconductor Gas Sensors Detection**

Gas sensor systems, sometimes called electronic noses, are devices that are able to capture and process signals generated by specific and reproducible interaction

processes with gas molecules, in one or more built-in sensitive layers. The development of this kind of devices has only been possible by the systematic production and characterization of new sensing materials, the availability of fast and sensitive electronic measuring systems and the fast growing knowledge in information theory to analyse multidimensional complex data. When the sensing layer and the electronic circuitry are integrated in the same chip, the device can be made very small and the production cost significantly lowered. There are already commercial gas sensor devices used for identification of specific contaminants or common mixtures. However much has yet to be done in order to improve sensitivity, selectivity and production cost of these devices.

The critical part of the sensor systems are the sensor elements, since a sensor array cannot produce better information than that contained in the sensors' responses. In order to make sensor systems portable, cheaper or usable for monitoring of air quality, sensor elements should: require low power for operation; be compatible with a simple sampling system or even have no need for one; have no need for external carrier or reactant gases; be made small and if possible compatible with microelectronic technologies; have reversible and reproducible responses; should have adequate sensitivity and have response times lower than one minute and long term stability if used in continuous operation or response times of a few seconds and short warm-up time if used for single gas analysis. It would also be useful to have sensors insensitive to ambient temperature and to the most common variable compounds of air, especially water vapour; with reproducible production characteristics; without hysteresis or drifts; with linear responses, fast recovery times and long lifetimes.

In general, semiconductor devices like Schottky diodes, MOS capacitors or field effect transistors can be made gas sensitive by using catalytically active materials such as platinum (Pt), palladium (Pd) or iridium (Ir) as Schottky or gate contacts. Lundstrom

*et al.* (Lundstrom *et al.*, 1975) started research into this direction in 1975 investigating the hydrogen sensitivity of silicon based MOS devices with palladium electrodes. Later a CO sensor of Si-MOSFETs was fabricated and its sensitivity was attributed to the porosity of the Pd gate electrode material (Krey *et al.*, 1983). Nevertheless, a severe limitation of Si devices on their inability of working continuously at temperatures higher than 250°C hindered the application at higher temperature. A more recent version, featuring a hybrid suspended gate electrode and a passive reference transistor has been described by Eisele and co-workers (Zimmer *et al.*, 2002). For more details about Si-MOS sensors, the interested reader is also referred to the extensive review by Crocker (Kreisl *et al.* 2005; Crocker *et al.*, 1991). Staying within the narrow temperature limits set by the silicon semiconductor material, H<sub>2</sub> was the only gas that could be detected by room-temperature operation.

In order to overcome this limitation, Lundstrom and co-workers (Arab *et al.*, 1993) later introduced MOS sensors fabricated on bulk SiC wafers with catalytic platinum electrodes (Pt-MOSiC). It has been proven that such MOSiC devices can be operated continuously at temperatures up to 800°C even in harsh environments such as combustion atmospheres (Lloyd Spetz *et al.*, 1997; 1998). Due to the enhanced catalytic efficiency at elevated temperatures, not only hydrogen but also a range of hydrocarbon species and NO<sub>2</sub> could be detected (Arab *et al.*, 1994; Lloyd Spetz *et al.*, 2000; Schalwig *et al.*, 2002, Jennifer *et al.*, 2005). Pioneering work on semiconductor gas sensors for combustion gas monitoring purposes was earlier performed by Lloyd Spetz and co-workers (Lloyd Spetz *et al.*, 1997; Lloyd Spetz *et al.*, 2000). This group has performed extensive investigations into silicon carbide (SiC)-based devices such as metal oxide semiconductor (MOSiC) capacitors, Schottky diodes (MISiC) and field effect transistors. Gas sensitivity was induced using catalytically active materials such as Pt, Pd and Ir as contact or gate metallisation materials. Such sensors have been shown to have millisecond response times (Tobias *et al.*, 1999) and are capable of

working at operation temperatures up to 800°C. Sensitivity towards hydrogen-containing molecules like molecular hydrogen and various hydrocarbon species was explained along the same lines of argument as those developed for the corresponding silicon devices (Schalwig *et al.*, 2002; Eriksson *et al.*, 1997; Fogelberg *et al.*, 1995). SiC devices exhibit a number of properties which make them less desirable for technical applications. Technical drawbacks are that the processing, particularly of SiC field effect transistors, is inherently complicated, requiring high-temperature implantation ( $T_i > 400^\circ\text{C}$ ) and very high-temperature post-implantation annealing steps ( $T_a > 1300^\circ\text{C}$ ). In addition, sensor chips fabricated from small pieces of bulk SiC substrates are hard to assemble and interconnect on ceramic heater substrates that form the backbone of commercial exhaust gas monitoring devices.

Although the number of materials used to implement this kind of devices is large, this work will be centered in studying the ones based on semiconductor properties and more specifically in the use of GaN as sensing materials. These Semiconductor Gas Sensors (SGS) present the property of changing the conductivity of the sensing material in the presence of a determinate gas (Feng *et al.*, 1994). The working temperature at which these devices are more efficient, can vary depending on the gas atmosphere and on properties of the sensor material selected in each case. At temperature range from 200 to 800 °C, far from room temperature, it is necessary to implement a heating system in sensor devices. A simple SGS will be composed of a substrate (where the sensor material will be supported), the electrodes (to measure the conductivity changes) and the heater (to reach the optimum sensing temperature) as showing in Fig. 1.1. Sensor electrical output signal, as well as input (heating power) is processed by a whole sensor system that usually includes a microprocessor (see Fig. 1.2). Despite its simplicity and cheap production, SGS usually exhibit drifts and variation in its behaviour. Therefore SGS are not so well established and nor modeled like other electronic devices. These problems are related with structural parameters of

the sensing material as well as device design. Nowadays these problems are known as the four s: sensitivity, selectivity, stability, and smart consumption (Cabot, 2000; Cirera, 2000).

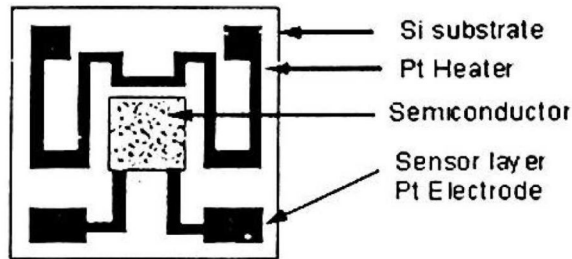


Fig. 1.1: Simple scheme of SGS with Si substrate, electrodes and heater resistance (Cirera, 2000).



Fig. 1.2: Gas sensor system that includes electronics for signal processing. [Figaro, 2000].

More recently, similar results were also obtained on GaN-based Schottky diodes (Schalwig *et al.*, 2001). As such GaN diodes can be grown as thin films on insulating sapphire substrates, single sensor devices as well as complex sensor arrays can be realized much more easily than in the case of MOSiC devices using straightforward planar technologies. Later similar kinds of devices were also realised on the basis of wide-bandgap III-nitride materials such as GaN and  $Al_{1-x}Ga_xN$  heterostructures (Schalwig *et al.*, 2002a; b; c). In the meantime, such wide-bandgap sensors have found a variety of applications, most of them relating to applications in

hot and corrosive environments such as exhaust and fuel gas monitoring (Schalwig et al, 2004; Wingbrant *et al.*, 2003a; b). Efforts made nowadays in SGS research field is to solve the problems that these materials can present. There are four parameters we should improve in order to obtain an accurate device: sensitivity, selectivity, stability and smart consumption (Cabot, 2000; Cirera, 2000).

### **1.2.1 Sensitivity**

This is the device characteristic of perceiving a variation in physical and/or chemical properties of the sensing material under gas exposure. In order to improve it, it will be of great interest to work with the most appropriate sensing material in every case, and reach its optimum detecting temperature. As suggested by several authors (Xu, 1990; Šundae, 1998; Shimizu, 1999; Williams, 1999), working with nanoscaled materials will give a higher surface area in front of gas. Taking into account that sensing reactions take place mainly on sensors layer surface, the control of semiconductor particle size will be one of the first requirements for enhancing the sensitivity of the sensor.

### **1.2.2 Selectivity**

A second difficulty in the development of SGS is its low selectivity; this kind of sensors exhibits good sensitivity to a broad variety of gases, hence it is difficult to distinguish them. This problem, usually called *interfering discrimination* is extremely important because when detecting CH<sub>4</sub> in an explosion alarm, few ppm of CO can produce a similar signal in sensor that methane have at level of explosion. Furthermore most part of gases (CO, CH<sub>4</sub>, O<sub>2</sub>, H<sub>2</sub>...) and volatile organic compounds –VOC-

(methanol, ethanol ...) can be detected with SGS. Several approaches were developed to overcome this difficulty.

First, the use of filter allows distinguishing gases by means of the interception of interfering gas by filters. Nowadays two families of filters are used. One is the passive filter that consist of a porous media (like charcoal in domestic SGS or alumina in automotive SGS) that inhibit diffusion of macromolecules (VOC, hydrocarbons) (Feng, 94; Morooka, 99; Schweizer-Berberich, 99), allowing only smaller molecules to reach SGS sensing surface. The other is the active filter consisting of catalytic metals (Pt, Pd) that burn volatile compounds.

Another approach was the use of doped sensing materials that are much more sensitive to one gas than others. The recent introduction of micromechanised substrates allows working in pulsed-mode heating. These substrates reach thermal stability in milliseconds. As the activation energy of gas/sensing-layer reaction is different for every gas, maximum temperature sensitivity is different too.

### **1.2.3 Stability**

One of the most desired characteristics in sensors is that these sensors give a reproducible signal after use. As described, SGS are based on physic-chemical surface and bulk reactions on nanometric crystalline grains at working temperatures of about 400°C. Such device is a complex system that usually exhibit great instabilities; key points for the understanding of lack of reproducibility are:

- physics and chemistry of surfaces still under development
- high working temperatures that enable gas/surface interaction

In order to overcome these extreme conditions, different strategies were developed. First, as the origin of the drifts is due to gas/sensing-material interaction, many efforts are devoted to improve material stability by means of reliable production procedures and appropriate annealing/firing treatments. The main idea is to apply thermal treatments ranging from 400°C to 1000°C for 1 to 8 hours- to avoid instabilities during working life it is continuously heated at 200°C-400°C. Nevertheless these thermal treatments are time consuming and produce grain growth. As pointed out, this growth is not desired as it will effect the device sensitivity. Another strategy to improve stability consists in applying surface treatments on sensing material. Several authors apply reducing treatments on surface before starting the measurements, and some sensing materials, such as  $WO_3$  (Williams, 1998), surface treatments consist of applying a fast thermal treatment (700°C during few minutes). In fact, most SGS manufacturers keeps sensors continuously heated about a week (or suggest to do) to avoid a first stage of instabilities (Mics, 2000; Fis, 2000; Figaro, 2000).

#### **1.2.4 Smart power consumption**

As seen above, SGS are devices that need to be heated continuously at very high temperatures. SGS's used to be heated between 200°C and 450°C, this will consume about 1W power, causing problem for portability. Nevertheless the use of sensors which are able to work with small portables batteries for domestic applications would be more interesting. Different strategies are being developed to overcome this difficulty. The use of dopants reduces the working temperatures. In  $SnO_2$  domestic gas sensors for CO, maximum sensitivity temperature is reduced from 450°C to 250°C when doped with palladium (Schweizer-Berberich, 1996). Such reduction of temperature approximately halves the power consumption. Although this improvement is important, industrial developments of sensors tend to develop more intelligent

substrate designs. Companies like Capteurs and Fis used smaller and thinner alumina substrates. This kind of sensors has a consumption of about 0.4 W (Fis, 2000; Capteurs, 2000). Nevertheless, the most interesting approaches were developed by the introduction of both micromachined silicon substrates and bead designed sensors. As pointed out in Fig. 1.2, micromachined silicon substrates have a very small mass and hence the power required for heating it is reduced. Advanced designs of micromachined substrates only consume about 30 mW (Mics, 2000). Similar values are obtained by bead design of Fis (Fis, 2000).

### **1.3 Mechanisms of gas sensing**

There are two major mechanisms by which we can sense the presence of a gas: (a) calorimetric detection, which measures gas concentration vs. temperature rise produced by the heat of reaction on catalytic surface; and (b) detection due to the change of electrical parameters, such as the change in electrical conductivity produced by the adsorption or reaction of gases on the solid surfaces. These two mechanisms are extensively reviewed by Grundy and Jones, (Grundy & Jones, 1976). It is well known that the atoms at the surface of a solid could not fully satisfy their valences. This phenomenon leads to a permanent force acting inward. So the adsorption of surrounding gas molecules will reduce the surface energy of the solid. One can distinguish two types of adsorption. (a) Physisorption: weak attraction followed by gas adsorption due to Van der Waals forces; which is characterized by a low heat of adsorption. (b) Chemisorption: in the case of high surface energy, the gas may become adsorbed through an exchange of electrons with the surface, i.e. forms chemical bonds. The heat of the latter is higher than that of the former one. Catalytic effects play an important role in the field of gas detection because catalytic processes not only control the rate at which a chemical reaction approaches equilibrium (response time) but also affect sensitivity and selectivity. An ideal catalyst is one, which

increases the rate of the gas-surface interaction without being permanently affected itself (Lundstrom *et al.*, 1989). In sensor technology two types of catalytic materials are usually used: metals and semi conducting metal oxides. In metals the electrons involved in chemisorption are the free electrons of the incomplete d-band. Thus one can understand why the noble metals (Pt and Pd) are the most active catalysts, as they possess a partially filled d-band. On the other hand the semi conducting metal oxides contain lattice defects due to an excessive or deficit of oxygen in the lattice. The association of electrons with these defects, following chemisorption, allows a certain change of the electrical conductivity of the oxide. In the case of metals, there is also a certain change of electrical conductivity due to the chemisorption of gases. But these changes are very small because of the high number of conduction electrons and therefore difficult to measure.

#### **1.4 Objective**

The aim of this study is to address the utilization of catalytic metal such as Pt, Pd, Ni and Ag in gas sensor device. By causing the excellent physical and chemical properties of GaN- based metal to the case of catalytic device, we can establish a comparable or better gas sensing device to those produce a SiC, GaAs and Si based material. This work will be study all of these flowing:

- 1- Study the sensing properties of M/GaN and AlGa<sub>N</sub> towards N<sub>2</sub>, H<sub>2</sub> and CH<sub>4</sub> gases.  
(M= catalytic metal)
- 2- The effect of annealing and operating temperatures on gas sensing properties of M/GaN and M/AlGa<sub>N</sub> sensors.
- 3- The effect of type of catalytic metals, Pt, Pd, Ag and Ni on gas sensing properties of GaN and AlGa<sub>N</sub> devices.
- 4- The effect of surface morphology on gas sensing properties of GaN and AlGa<sub>N</sub> devices.

## 1.5 Outline of the thesis

The main portion of this work is to study and develop new materials for gas sensing elements starting from the knowledge in thin film production using sputtering method available in the School of Physics, Universiti Sains Malaysia. Some concepts used on sensor development and specifically on chemical sensors and gas sensors' research are described in Chapter 2. The reason to start studying gallium nitride with noble metals response to gases is also explained. In the following chapter, the properties and characteristics of GaN are presented. Different technological designs developed in this thesis are described in detail, and the material procedure for GaN is presented in Chapter 4. Chapter 4 also described the home made chamber setup built in our laboratory for gas sensing characterization and the methodology to carry out GaN sensors devices characterization. The performance properties of GaN for gas sensors are studied and compared in Chapter 5. The results of the surface morphology of different gas sensors are discussed on Chapter 6. And finally, Chapter 7 summarizes the main conclusions of this work and also points some directions for future research that may be carried out in our laboratory at the Universiti Sains Malaysia.

## CHAPTER [2] CHEMICAL SENSORS

### 2.1 What is a sensor?

A definition given by Jacob Fraden in the *Handbook of modern sensors* (Fraden, 1997), states that “a sensor is a device that receives a signal or stimulus and responds with an electrical signal”. The reason for the output of a sensor to be limited to electrical signals is related to the present development of signal processing that is almost exclusively performed using electronic devices. Given this definition, a sensor should be a device that receives a physical, chemical or biological signal and converts it into an electric signal, that should be compatible with electronic circuits. This definition may also be supported from the etymological origin of the word sensor. Sensor seems to come from the word *sense* given that usually sensor devices try to mimic or reproduce human senses' characteristics.

In the biological senses the output is also an electrical signal that is transmitted to the nervous system. Another term with a meaning similar to sensor is transducer. Sometimes transducer is used as a synonym for sensor, as is the case in a series on sensors edited by Göpel *et al.* (Göpel *et al.*, 1989; 1990; 1991; 1992). Nevertheless, transducer will be distinguished from sensor throughout this report. Transducer will be used to designate any device which converts a stimulus into any other form, whether electric or not. In this sense a sensor is only the transducer that produces an electric output.

A sensor may be composed by a series of transducers responding in the end with an electrical output, in which case, given the above definition, the last transducer in the series could also be termed a sensor. A transducer may also be called sensor element, when it is part of a sensor. Usually sensors are part of larger complex

systems, made by many other transducers, signal conditioners, signal processors, memory devices and actuators.

The components of a sensor system may be grouped in three different units. The first is the sensor unit, the second is the modifier or signal processor and the third is the output transducer. The second class of components receives the electrical output of the sensors and transforms it into a more suitable form, e. g., amplifying, converting to digital form or linearizing the signal. The third class, termed the output transducer, converts again the electrical signal into a non-electrical parameter. When this last parameter can be perceived by the human senses the output transducer is called a display and the whole system may be called a measuring system. If the output transducer is used to cause some action it is called an actuator and the whole system is a control system. Both control and measuring systems may be included in a larger group of the information processing systems. These are systems that gather data from a variety of sources and process it in order to produce usable information.

## 2.2 Liquid Sensors

Liquid is a state of matter in which a sample of matter (flows and can change its shape and is not easily compressible and maintains a relatively fixed volume. A sample of bromine ( $\text{Br}_2$ ) at room temperature is shown in Fig. 2.1 below. As may be seen in the microscopic view of liquid bromine:

- Liquids are made up of very small particles (atoms, molecules, and/or ions).
- The particles that make up a liquid (are close together with no regular arrangement and vibrate, move about, and slide past each other).

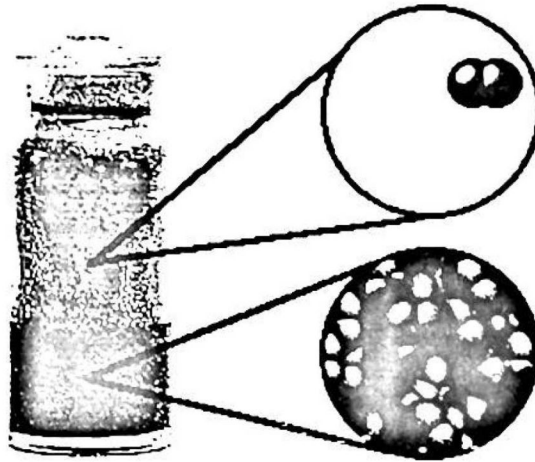


Fig. 2.1: This bottle contains both liquid bromine [ $\text{Br}_2(\text{l})$ , the darker phase at the bottom of the bottle] and gaseous bromine [ $\text{Br}_2(\text{g})$ , the lighter phase above the liquid]. The circles show microscopic views of both liquid bromine and gaseous bromine.

Sensors for common Industrial Use Cryogenics are also available for materials such as water, liquid oxygen, liquid hydrogen, liquid carbon dioxide (liquid  $\text{CO}_2$ ), liquefied natural gas (LNG), liquid argon, liquid propane, liquid butane and pH.

The pH scale corresponds to hydrogen ion concentrations from  $10^0$  to  $10^{-14}$  moles per liter and, therefore, systems for pH control cover an extreme range. No other common measurement covers such a tremendous range. In addition, the measuring electrodes can respond to changes as small as 0.001 pH, and, therefore, systems for pH control are also extremely sensitive.

The design of these pH control systems is complicated by pH being a logarithmic function of concentration. For example, if a certain amount of base added to a solution of strong acid would increase the pH from 2 to 3, increasing the pH further to 4 may only require 10% of the original volume. If it is necessary to increase the pH to 5, only 1% of the original volume is required, and for pH 6, only about 0.1%. Therefore, taking a waste stream from pH 2 to 7 can be a difficult control problem.

a) The pH control system typically has the following equipment:

- pH sensor.
- Analyzer.
- Recorder.

In addition, there is typically a control panel with an indicator, starters, and controls for chemical metering pumps, high/low pH alarms, switches, and mixer motor starters.

(1) *pH/ORP Sensors.* A pH sensor is an electrochemical device that produces a voltage proportional to the pH/ORP of the solution into which it is placed. Definition of ORP, ORP is an abbreviation for Oxidation-Reduction Potential. ORP probes are used when agents other than hydroxide precipitating agents are used. The following things should be done when selecting the proper pH/ORP sensors:

- Determine mounting requirements and sensor body style.
- Ensure that the measuring electrode fits process temperature, chemistry, and physical parameters.
- Determine if an automatic temperature compensator is required (becomes critical as the temperature changes from 25°C, or the pH from 7.0).
- Determine what accessory hardware is required to mount a particular type of sensor.
- Determine cabling requirements to connect the sensor to the analyzer.

ORP displays should be capable of reading both positive and negative milli volt values.

(2) *pH Analyzers.* The key function of the pH analyzer is to receive the voltage signal from the pH sensor and convert it to a pH value. The pH scale has an equivalent y mV scale. The mV scale ranges from +420 to -420. At a pH of 7.0 the mV value is zero. Each pH unit change corresponds to a change of + or -60 mV. As the pH becomes more acidic, the values become greater. For most processes, a pH analyzer is required to do more than simply display a pH value. Based on specific pH set points, the analyzer also transmits signals to recorders or a control system that activates (or deactivate) alarms, valves, or pumps.

b) For batch systems, the pH control device can be relatively simple with only on–off control provided via a solenoid or air-activated valves. For continuous flow systems, pH control is more complicated because of the greater potential for fluctuation in both flow and contaminant concentration.

c) Because of the introduction of microprocessor-based technology many industrial instrumentation controllers and analyzers, now use configurable algorithms to characterize their function curves.

d) Suggested references for further reading for design of pH control are Water Environment Federation (Federation, 1994; 1993; Hoyle, 1976; Cushnie, 1984; Hoffman, 1972).

## **2.3 GaN Gas Sensor**

### **2.3.1 GaN Gas Sensor Science and Technology**

The sensing capabilities of the catalytic metal gate with a wide bandgap GaN semiconductor metal semiconductor field effect transistor (MESFET) and modulation doped field effect transistor (MODFET) transducers are advantageous for high temperature measurement of carbon monoxide in hydrogen.

Fig. 2.2 shows the comparison between energy band gap for different semiconductors and Table 2.1 lists the different properties of semiconductors. The choice of the catalytic metals for the device is based on the metals used in FET detectors for lower temperature applications and based on data for metals used in the three-way automobile catalytic converter: platinum, palladium/silver and rhodium.

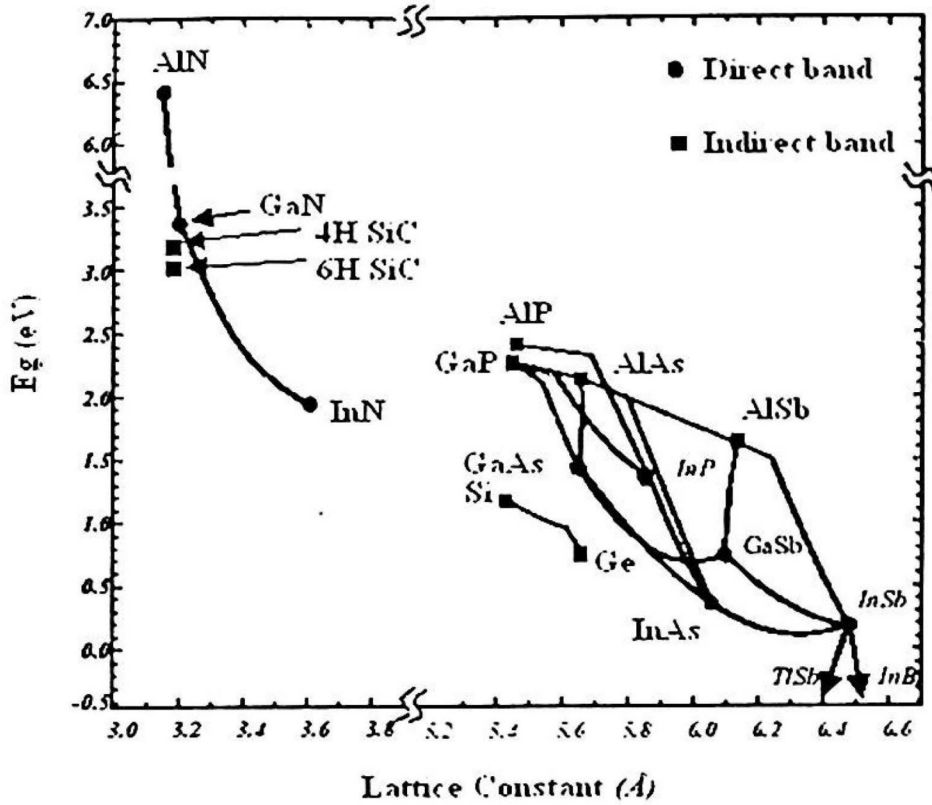


Fig. 2.2: Energy band gap for semiconductors (Pearton *et al.*, 2002).

Table 2.1: Properties of semiconductors (Pearton *et al.*, 2002).

	AlN	GaN	InN	6H-SiC	4H-SiC	Si
300K bandgap (eV)	6.2	3.4	1.9	3.0	3.23	1.12
Lattice constant a (Å)	3.112	3.189	3.545	3.081	3.073	5.431
Lattice constant b (Å)	4.982	5.189	5.703	15.117	10.053	5.431
E (MV/cm)	> 3	~3	---	~3	~3	0.25
Electron effective mass ( $m_e$ )	---	0.2	0.11	$2.6*m_e$	$0.29*m_e$	$0.9*m_e$
Hole effective mass ( $m_h$ )	---	0.8	$0.5*m_h$	~1	~1	$0.2*m_h$
n (refractive index)	2.15	2.67	2.9	2.7	2.712	3.5
Thermal Conductivity(W/cmK)	2.0	1.3	0.8	~3.4 R.T	~3.4 R.T	1.48
Melting point (°C)	3000	>1700	1100	>1800	>1800	1683

## 2.4 GaN Gas Sensing Mechanism

### 2.4.1 Gas Mechanisms

Physisorption is the weakest form of adsorption to a solid surface and is essentially maintained by Van der Waals interactions. Given the unselective character

of Van der Waals interaction, sensors based on physisorption processes usually exhibit sensitivity to a wide range of gaseous species. Chemisorption, on the other hand, is a stronger interaction, that shows a higher selectivity. In this kind of interactions, adsorbates form chemical bonds with the surface atoms and thus the electronic structure of both the adsorbate and the surface are modified. Chemisorption is usually promoted by surface defects. By a defect, one generally means any region where the microscopic arrangement of the particles differs from a perfect crystal. The interaction mechanisms between the gas phase and the sensing material involve mainly physisorption, chemisorption, surface defects, bulk defects or three phase boundary processes.

According to this model, the sensitivity to various reducing and hydrogen or hydrocarbons gases can be traced back to the porosity of the metal gate. This porosity normally arises from mechanical stress in the metal layer and agglomeration of metal clusters caused by high temperature operation or high temperature annealing during device processing. For a porous gate, direct adsorption of the gaseous molecules or of follow-on products, formed by reaction on the metal surface, occurs on the top surface of the GaN layer as shown in Fig. 2.3. As these open areas are exposed to an oxygen-containing atmosphere during measurement and device processing, the GaN possibly will be oxidized so that the adsorption in the pores takes place on some form of non-stoichiometric Ga-oxynitride. As a consequence, the effects taking place in the pores of the metal layer can be explained in a similar way as those on metal surfaces. The adsorption leads to a change in the surface depletion layer in the non-metal-covered areas of the semiconductor material. Such a modulation occurs due to three different effects: firstly, by the creation or removal of surface dipoles directly associated with the adsorbed species. This effect is likely to dominate in the case of moderately electronegative gases such as nitrogen ( $N_2$ ) and carbon monoxide (CO) (CO was obtained from  $CH_4$  dissociation to carbon and hydrogen atoms, which then react with

oxygen to form CO first and CO<sub>2</sub> later). The second effect involves highly electronegative gas species such as oxygen or methane.

However, for methane (CH<sub>4</sub>), experimental studies report a decrease of the sensor resistance in the presence of CH<sub>4</sub> (Kohl, 2001). It is observed that at higher temperatures CH<sub>4</sub> detection is favourable than CO detection. Previous study assumed, based on reactive scattering results, two principle reaction pathways for CH<sub>4</sub>. The first involves the reaction with lattice oxygen and the second one the reaction with ionosorbed oxygen. The reaction of CH<sub>4</sub> with lattice oxygen leads to the creation of oxygen vacancies. Therefore, they can account for the resistance increase observed in the presence of CH<sub>4</sub> at higher sensor operation temperatures. Adsorption of such species leads to an electron transfer from the GaN to the adsorbate and, therefore, to an increased depletion layer in the underlying n-type semiconductor material. In the case of hydrogen (H<sub>2</sub>), a third effect occurs which is not related to the existence of pores in the metal layer and which, therefore, also appears in the case of continuous, non-porous gates.

With respect to the different molecular species considered above, hydrogen plays an outstanding role in that it is the only species able to diffuse through a dense noble metal layer into deeper lying layers of the semiconductor device – at least within the range of operating temperatures investigated – leading to hydrogen selectivity in the case of continuous and nonporous gate electrodes. The hydrogen sensitivity is normally explained by the formation a H-induced dipole layer at the interface of the GaN and the metal layer. As shown in Fig. 2.3, molecular hydrogen dissociates at the metal surface, penetrates through the bulk and builds up a dipole layer by chemisorption at the interface. The dipole moment is oriented out of the GaN leading to a negative voltage drop.

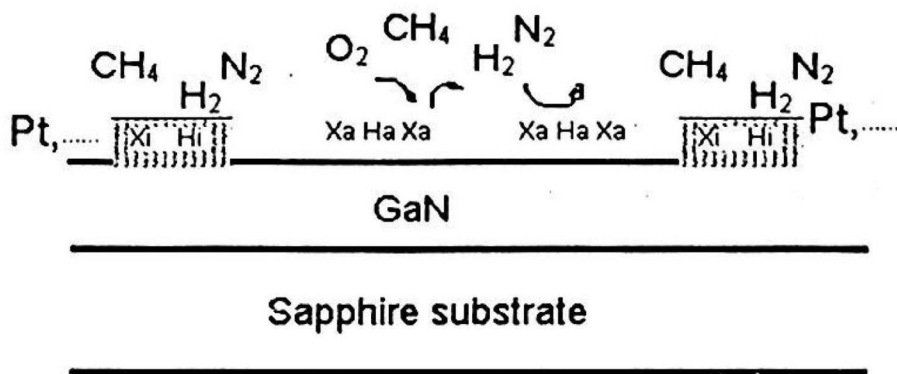


Fig. 2.3: Proposed gas sensing mechanisms underlying the function of catalytic metal gas sensor devices ( $H_{ads}$ ,  $H_i$ : adsorbed and interfacial hydrogen;  $X_a$ ,  $X_i$ : adsorbed and interfacial molecules).

Therefore, the dipole layer will also be balanced by a modulation of the depletion layer, which leads to a decrease in the Schottky barrier height. The modulation of the depletion layer is caused by both adsorption of hydrogen at the metal–GaN interface and chemisorption of gaseous species on bare GaN areas. In general, oxidizing gases lead to an increased depletion layer and as a consequence to a decreased out current, whereas sensor signals opposite in sign appear upon exposure to reducing gases like  $H_2$  or hydrocarbons.

## 2.4.2 Microstructures

The interaction of compact and porous layer with surrounding gases is rather different, as shown in Fig. 2.4. Porous layers are accessible to gases in the whole volume whereas compact layers only interact with gases at the geometric surface. The gas active surface of porous layers is therefore much larger than in the case of compact layers (Simon *et al.*, 2001). Additionally, the two layers differ in the way how gas-induced changes at the gas-active surface are transduced in a sensor output signal such as sensor resistance: in case of compact layer current flows through two resistances in parallel, one is being equivalent to the geometric surface which is affected by gas reactions, the other corresponding to the gas-unaffected bulk. The sensitivity of compact layers depends, therefore, strongly on the layer thickness: only

in case where the thickness of the electron depleted surface thickness is about the size of the compact layer, high gas sensitivity can be expected (Simon *et al.*, 2001). A small gas concentration can then work like a switch closing or opening the conducting channel.

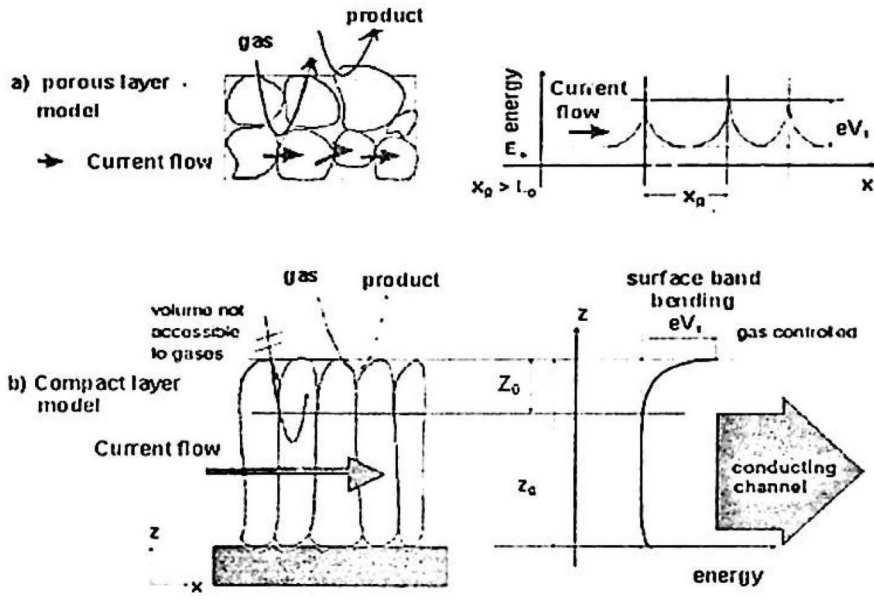


Fig. 2.4: Schematic representation of (a) porous and (b) compact sensing layer with geometry and energy band.  $X_g$  grain size,  $L_D$  Debye length,  $eV_s$  Band bending,  $z_0$  thickness of the depleted surface layer and  $z_g$  layer thickness (Simon *et al.*, 2001).

In case of porous layers the situation is different, each grain possess a surface depleted area and current has to pass through the intergranular contacts, the resistances of gas-unaffected bulk and surface-depleted areas are put in series. These two models, even though simplifying the real microstructures of gas sensors, show that the expected sensor characteristics of most thin film sensors are expected to behave differently from thick film sensors.

Due to the larger gas-active surface area of porous layers compared to compact layers, higher sensitivity and higher fullerene and thus altering of sensors is expected in case of porous layers (Simon *et al.*, 2001).

### 2.4.3 Hydrogen Sensing and Transduction

GaN sensors are generally operated in air in the temperature range between 200 and 400°C. At these temperatures it is generally accepted that the conduction is electronic; it is also accepted that chemisorption of atmospheric gases takes place at the surface of the GaN. The overall conduction in a sensor element, which will determine the sensor resistance, is determined by the surface reactions, the resulting charge transfer processes with the underlying semiconducting material and the transport mechanism from one electrode to the other through the sensing layer (the latter can even be influenced by the electrical and chemical electrode effects).

For example, it is well known and generally accepted that the effect of oxygen ionosorption as  $O^{-2}$  or  $O^{-}$  will be the building of a negative charge at the surface and the increase of the surface resistance. It is also considered that reducing gases like  $H_2$  react with the surface oxygen ions, freeing electrons (the sensing step) that can return to the conduction band. The transduction step, i.e. the actual translation of this charge transfer into a decrease of the sensor resistance, depends on the morphology of the sensing layer. The result is that, even for exactly the same surface chemistry, the dependence of the sensor resistance on the concentration of  $H_2$  can be very different for compact and porous sensing layers. Due to the fact that the final thermal treatment is performed at 600°C, the grains are just loosely connected. Accordingly, the best way to describe the conduction process is to consider that the free charge carriers (electrons for GaN sensor device) have to overcome the surface barriers appearing at

the surface of the grains (see Fig. 2.5). One can easily model the dependence of the resistance on the  $H_2$  concentration by making the following assumptions, supported by the already established knowledge in the field:

- The reaction of  $H_2$  takes place just with the previously adsorbed oxygen ions (Barsan & Weimar, 2003; 2001), (well documented for the temperature and pressure range in which the gas sensors operate).
- The adsorption of  $H_2$  is proportional to the  $H_2$  concentration in the gas phase (quite reasonable but never really experimentally proved).

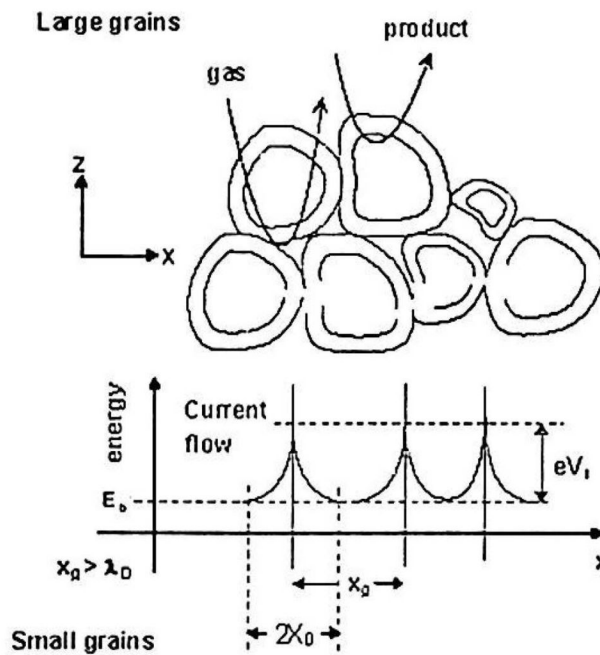


Fig 2.5: Schematic representation of a porous sensing layer with geometry and energy band.  $\lambda_D$  is the Debye length,  $x_g$  is the grain size and  $x_0$  is the depth of the depletion layer (Barsan & Weimar, 2003; 2001).

#### 2.4.4 Current/Voltage (I-V) Characteristics

A good Schottky barrier usually is made from high-mobility semiconductors possess  $J/V$  characteristics given by the thermionic-emission theory provided the

forward bias is not too large so that saturation current  $J_s$  obtained is small enough to acquire higher Schottky barrier height. The  $J/V$  relationship is given as:

$$J = J_s \{ \exp(qV/kT) - 1 \} \quad (2.1)$$

where  $J$  is the current density (current/unit area) (Rhoderick and William, 1988) and

$$J_s = A^* T^2 \exp\{-q(\phi_b - \Delta\phi_n)/kT\} \quad (2.2)$$

For convenience, we shall call  $\phi_b - \Delta\phi_n$  the effective barrier height  $\phi_e$ .  $A^*$  is called the effective Richardson constant. The value of Richardson constant depends on the effective mass.

Indeed, in practice diodes never satisfy the ideal equation (2.1) exactly, but can be more closely described by the modified equation (Rhoderick and William, 1988)

$$J = J_s \exp(qV/nkT) \{ 1 - \exp(-qV/kT) \} \quad (2.3)$$

where  $n$  (which may depend on temperature) is approximately independent of  $V$  and is greater than unity. There are many possible reasons why  $n$  should exceed unity, the most common being a bias dependence of  $\phi_b$  and  $\Delta\phi_n$ . For values of  $V$  greater than  $3kT/q$ , eq (2.3) can be written in the simpler form

$$J = J_s \exp(qV/nkT) \quad (2.4)$$

By simplifying into this form (eq. 2.4), a plot of  $\ln J$  against  $V$  in the forward direction should give a straight line except for the region where  $V < 3kT/q$ . In practice one always measures the total current  $I$  rather than the current density  $J$ , and the determination of  $J$  necessitates an accurate measurement of the area  $A$ . The advantage of retaining the more exact form of eq (2.3) is that a plot of  $\ln[I/1 - \exp(-qV/kT)]$  against  $V$  should give a straight line for all values of  $V$ , not only for  $V < 3kT/q$  but for negative (i.e. reverse) values as well. The determination of barrier height from  $I/V$  characteristics is only reliable if one can be confident that the current is determined by the thermionic emission theory. For this to be so, the forward